

## Intermodulation atomic force microscopy

Daniel Platz, Erik A. Tholén, Devrim Pesen, and David B. Haviland<sup>a)</sup>  
*Nanostructure Physics, Royal Institute of Technology, SE-10691 Stockholm, Sweden*

(Received 21 January 2008; accepted 26 March 2008; published online 15 April 2008)

A mode of atomic force microscopy (AFM) is demonstrated where an oscillating AFM cantilever having linear response is driven with two frequencies in the vicinity of a resonance. New frequencies in the response, known as intermodulation products, are generated when the linearity of the cantilever response is perturbed by the nonlinear tip-surface interaction. A rich structure of the intermodulation products is observed as a function of the probe-surface separation, indicating that it is possible to extract much more detailed information about the tip-surface interaction than is possible with the standard amplitude and phase imaging methods. © 2008 American Institute of Physics. [DOI: 10.1063/1.2909569]

The sensitivity and utility of atomic force microscopy (AFM) were considerably enhanced by the introduction of resonant detection<sup>1,2</sup> or “tapping mode” AFM.<sup>3</sup> In the standard realization of tapping mode AFM, a probe consisting of a cantilever with a sharp tip is driven near the fundamental eigenmode of the cantilever at frequency  $f_0$ . When the probe is brought close to a surface, the atomic forces between the tip and the surface are detected by measuring a change in the amplitude and phase of the cantilever oscillation at the frequency that the cantilever is driven. Attempts to extend tapping mode AFM and extract more information regarding the surface properties include analyzing the cantilever oscillation for higher harmonics of the drive frequency.<sup>4–6</sup> These harmonics do not generally coincide with higher order eigenmodes of the cantilever, and therefore, response is very small. Special cantilevers with flexural eigenmodes at or near the harmonics of the fundamental,<sup>7</sup> or higher frequency torsional eigenmodes have also been investigated.<sup>8</sup> Other techniques employ two drive frequencies, one at each of the two lowest eigenmodes of the cantilever while measuring the response at both drive frequencies.<sup>9,10</sup> Here, we demonstrate a method to probe the tip-surface interaction using only the fundamental eigenmode of a cantilever, where a highly linear response of free cantilever oscillation is weakly perturbed by the nonlinear tip-surface interaction, causing new frequencies to appear in the response.

The sensitivity of resonant detection is improved when the resonator (oscillating cantilever) has a weak damping, so that a high quality factor  $Q$  is achieved.<sup>11</sup> High  $Q$  resonators build up large amplitude oscillation on resonance, which implies that the restoring force should be a highly linear function of the coordinate describing the displacement from equilibrium. The tip-surface force, on the other hand, is not a linear function of this coordinate. When this nonlinearity is strong enough (i.e., probe close enough to the surface), strong distortion of the resonance curve and bifurcation, or the appearance of multi-valued oscillation states, occur.<sup>12,13</sup> However, a very weak nonlinearity, which barely distorts the resonance curve, can be detected by measuring intermodulation products (IMPs).<sup>14</sup> Intermodulation is a phenomenon in nonlinear systems driven with more than one frequency, where the nonlinearity causes the generation of new frequen-

cies in the response, which are not present in the drive. In many engineering contexts, intermodulation is considered an undesirable effect and intermodulation measurements are used for characterization of signal distortion due to nonlinearity. Here, we use intermodulation in an advantageous way to realize a very sensitive, high information bandwidth mode of AFM, which we call intermodulation AFM (IMAFM).<sup>15</sup>

In Fig. 1, we compare the response of a linear resonator and a nonlinear resonator when driven with two frequencies. The linear resonator [Fig. 1(a)] shows response only at the two drive frequencies,  $f_1$  and  $f_2$ . In the nonlinear resonator [Fig. 1(b)], new frequencies are present in the response, which are the IMPs. Following the usual convention, we denote the IMPs by their order as described in Fig. 1(b). For the realization of IMAFM demonstrated here, we study the odd order IMPs, which form a series of peaks near the resonance with spacing  $n\Delta f = n(f_2 - f_1)$  from the two drive frequencies ( $n$  is an integer).

To realize IMAFM, we used a Veeco multimode AFM and Nanoscope IV controller equipped with a signal access module together with several pieces of auxiliary equipment. The signal used to drive the cantilever consisting of two frequencies was synthesized with two arbitrary waveform

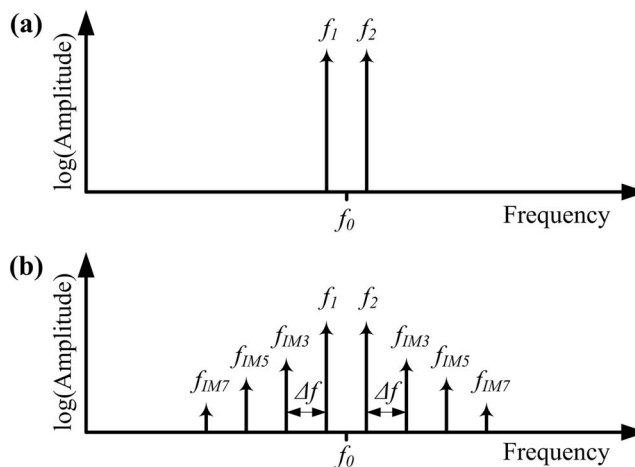


FIG. 1. (a) The linear response of the resonator away from the surface. When driven with two frequencies,  $f_1$  and  $f_2$ , the linear system responds with oscillation at  $f_1$  and  $f_2$ . (b) When close to the surface, nonlinear tip-surface interactions generate IMPs of many orders.

<sup>a)</sup>Electronic mail: haviland@kth.se.

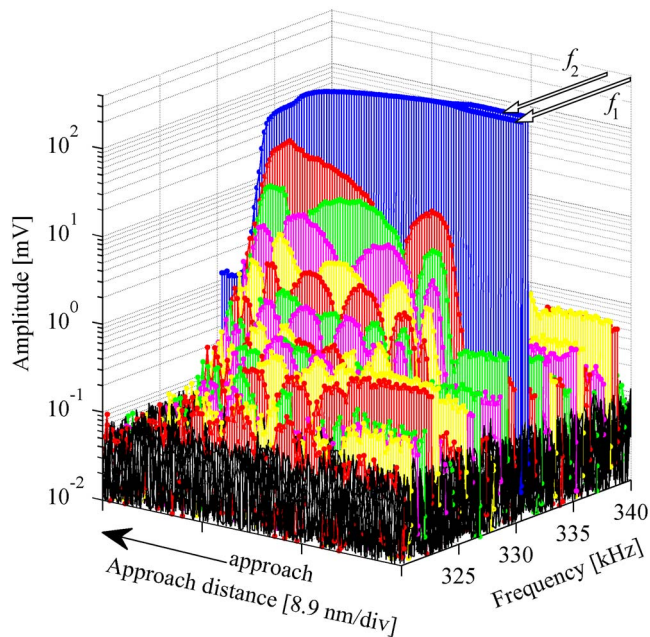


FIG. 2. (Color online) The frequency spectra of the cantilever response are plotted as the surface is approached. Many intermodulation peaks of higher order can be seen, where the amplitude of each peak is uniquely dependent on the tip-surface separation.

generators (AWGs) and a summing preamplifier. A data acquisition card (DAC) was used to measure the cantilever response by capturing the raw detector signal from the split quadrant photodiode in the AFM head. The clocks of both AWGs and the DAC were phase locked to the same 10 MHz signal. While scanning, lines of data were captured on the trace, and during the retrace they were parsed and Fourier transformed to extract the IMP amplitudes at different tip positions. When scanning the test samples, our IMAFM system was run in parallel with the Nanoscope system, using the feedback and scanning controls of the Nanoscope IV controller. In this way, we could compare IMAFM with the standard amplitude and phase imaging methods. The AFM probe used here was a relatively stiff Si tapping mode probe with a beam-type cantilever (RTESP-300, nominal spring constant 40 N/m) having a resonant frequency  $f_0=330.8$  kHz and  $Q=633$ , or mechanical bandwidth  $B=f_0/Q=523$  Hz. It was driven by a small piezostack built into the probe holder. The AFM probe was cleaned in an oxygen plasma prior to measuring. Measurements were performed at room temperature in air on Si chips with a special surface chemistry described below.

Figure 2 is a three-dimensional plot showing the spectra of the cantilever response (log amplitude versus frequency) as the cantilever is approaching the surface. When the tip is far from the surface, at the right hand side of Fig. 2, the response spectrum has two dominant peaks, which are the two drive frequencies  $f_1$  and  $f_2$ . At this distance from the surface, the cantilever is undergoing free oscillation, unperturbed by the tip-surface interaction. The free oscillation response spectrum also shows a background of intermodulation peaks of many orders, which are visible above the noise floor. These background peaks are due to nonlinearities in the DAC and could be reduced with better quality electronics.

To clarify the origin of these background IMPs, we made a detailed study of the free cantilever response as a function of the drive amplitude. Sweeping two equal amplitude drive

signals  $f_1$  and  $f_2$  with fixed  $\Delta f$  through the cantilever resonance, we recorded the amplitude of the response at  $f_1$ ,  $f_2$ , and  $f_{IM3}$  (data not shown here). When the cantilever was driven near the resonance and undergoing large amplitude oscillations (detector signal amplitude  $>0.8$  V), a third order IMP could be seen above the background, which was generated by the nonlinear dynamics of the cantilever itself. However, at the oscillation amplitude levels used in the following (detector signal amplitude  $<0.4$  V), IMPs due to the cantilever itself were well below the background level of our detection system.

As the surface is approached (moving from the right to left in Fig. 2), the response spectra show a large increase in the measured IMPs, and the measured amplitude of these IMPs show much variation with the average probe-surface separation. By making  $\Delta f \approx B$ , a large number of IMPs can be measured in the response spectrum. In Fig. 2 with  $\Delta f=600$  Hz ( $B=523$  Hz), one can count as many as nine measurable IMPs, each with a unique dependence on probe-surface separation, and presumably containing a great deal of information about the exact nature of the tip-surface interaction. However, at this time, we lack a general theory of how to extract the tip-surface potential from this data.

Note that the optimal measurement bandwidth of IMAFM is given by  $\Delta f$ , which can be chosen smaller or larger than the mechanical bandwidth  $B=f_0/Q$  of the resonator. Smaller  $\Delta f$  will result in longer measurement time and, therefore, slower scanning speed, but small  $\Delta f$  will also give a larger number of IMPs within the frequency band of finite cantilever response. Here, we see how IMAFM optimally uses frequency space to extract information from the oscillator regarding the nonlinear perturbation. IMAFM has a much larger information bandwidth than standard tapping mode AFM, which records response at only one frequency. Thus, IMAFM represents an ideal approach to dynamic force microscopy, where the goal is to determine the functional form of the tip-surface interaction by analysis of the cantilever response.<sup>13</sup>

To more clearly show the structure of the IMPs versus probe-surface separation, we plot the amplitude of the cantilever response (linear scale) at the two drive frequencies and the first three odd IMPs (Fig. 3). Here, we see the response for both the approach and the retracting of the probe from the surface, which was done in one continuous ramp toward and away from the surface. The strong similarity of approach and retract for each curve demonstrates that the measured change in cantilever response is reversible, or nonhysteretic. Important for the sensitivity of AFM is the responsivity (i.e., slope of curves in Fig. 3) at first contact with the surface, which is similar in magnitude for the drive frequencies and the IMPs. However, the IMPs start from a low signal level and, therefore, a small change in IMP amplitude can be detected without saturation by using higher gain electronic amplifiers with appropriate filtering. The responsivity of the IMPs will depend on the choice of  $f_1$  and  $f_2$  relative to  $f_0$ , which was not optimized in this measurement.

To demonstrate the utility of IMAFM in imaging mode, we show an image of a special sample consisting of a protein monolayer adsorbed on to a smooth Si surface (Fig. 4). On this surface, a stripe pattern is exposed with a low energy (5 keV) electron beam in an electron beam lithography system. The exposure causes a chemical change in the surface where the electrons strike the protein monolayer but no

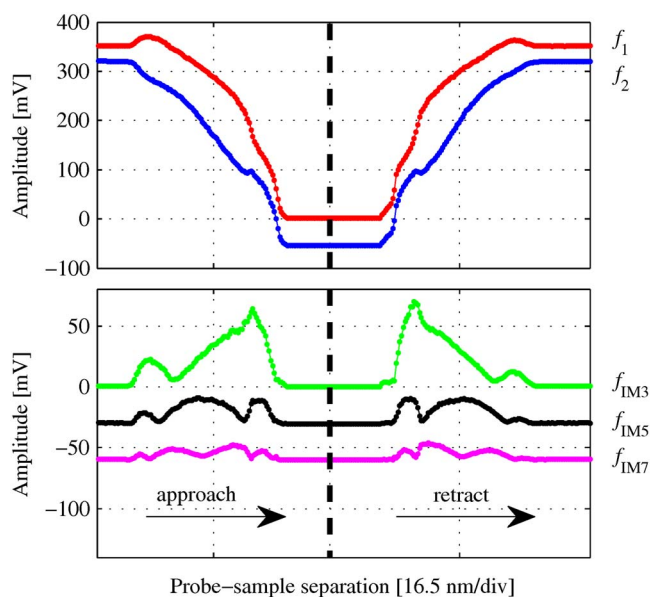


FIG. 3. (Color online) The amplitude of response at the two drive frequencies,  $f_1$  and  $f_2$ , and the first three odd IMPs. The  $f_2$ ,  $f_{IM3}$ , and  $f_{IM7}$  curves have been offset on the vertical axis for clarity.

change in topography.<sup>16</sup> We performed standard tapping mode height and phase imaging, where the feedback regulated the probe-surface separation to keep a constant amplitude of the cantilever response at the drive frequency as the tip was scanned over the surface. While scanning, the height image (i.e., feedback signal) was featureless, but we see in Fig. 4(a) how the exposed striped pattern can be seen in the phase image. Phase imaging is a well established technique for sensing very subtle changes in surface chemistry,<sup>17</sup> which cause a change in resonator damping.<sup>18</sup>

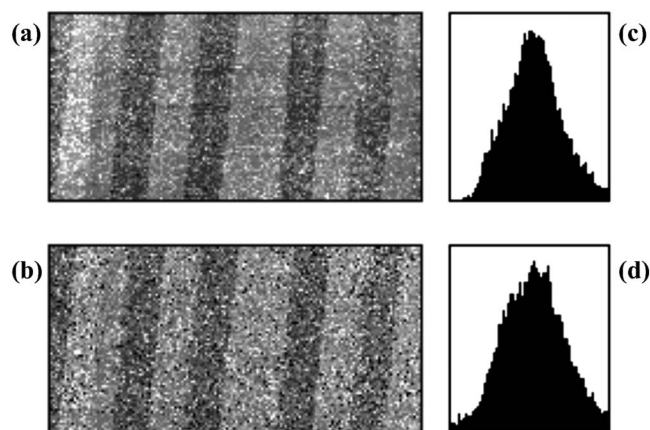


FIG. 4. A comparison of the phase image (a) of standard tapping mode AFM and the IM3 image (b) collected with identical feedback setup. The sample is a protein monolayer adsorbed on to a smooth SiO<sub>x</sub> surface. A striped pattern exposed with an electron beam causes a chemical change, but no change in surface topography. The histograms (c) and (d) show the distribution of grayscale values in (a) and (b), respectively. The scan width is 100  $\mu\text{m}$ .

In a second sweep over the same area using IMAFM, we simultaneously gathered several images by recording the amplitude of IMPs of higher orders. Figure 4(b) shows the image generated from the amplitude of IM3, which is somewhat noisier than the phase image, due to the lower signal level of IM3 in comparison with the phase. However, a comparison of the grayscale histograms [Figs. 4(c) and 4(d)] shows that the IM3 image has slightly better contrast than the phase image. We also found that imaging on IM3 was more stable and easier to use than phase imaging. When phase imaging, the contrast would often jump, presumably due to a small change in the cantilever resonance when impurities get stuck to the cantilever. The IM3 image appeared to be immune to such jumps.

These experiments demonstrate that IMAFM is an attractive alternative to tapping mode AFM. With further optimization of the technique, images can be acquired in a single scan with higher sensitivity and greater information content than the standard tapping mode AFM. In closing, we note that IMAFM can be performed by running the feedback directly from one or a combination of the IMPs, and that implementation of IMAFM can be greatly simplified in the present generation of AFMs where the modern controllers have a larger capacity for digital signal synthesis and processing.

This work was supported by the Swedish VR, Wennergren Foundation and used the Albanova Nano Fab Laboratory with equipment donated by the K A Wallenberg Foundation.

<sup>1</sup>Y. Martin, C. C. Williams, and H. K. Wickramasinghe, *J. Appl. Phys.* **61**, 4723 (1987).

<sup>2</sup>T. R. Albrecht, P. Grütter, D. Horne, and D. Rugar, *J. Appl. Phys.* **69**, 668 (1991).

<sup>3</sup>Q. Zhong, D. Inness, K. Kjoller, and V. B. Elings, *Surf. Sci. Lett.* **290**, L668 (1993); US Patent No. RE36,488 2000.

<sup>4</sup>R. W. Stark and W. M. Heckl, *Rev. Sci. Instrum.* **74**, 5111 (2003).

<sup>5</sup>M. Balantekin and A. Atalar, *Appl. Phys. Lett.* **87**, 243513 (2005).

<sup>6</sup>S. Crittenden, A. Raman, and R. Reifengerger, *Phys. Rev. B* **72**, 235422 (2005).

<sup>7</sup>O. Sahin, G. Yaralioglu, R. Grow, S. F. Zappe, A. Atalar, C. Quate, and O. Solgaard, *Sens. Actuators, A* **114**, 183 (2004).

<sup>8</sup>O. Sahin, S. Magonov, C. Su, C. F. Quate, and O. Solgaard, *Nat. Nanotechnol.* **2**, 507 (2007).

<sup>9</sup>N. F. Martinez, S. Patil, J. R. Lozano, and R. Garcia, *Appl. Phys. Lett.* **89**, 153115 (2006).

<sup>10</sup>R. Proksch, *Appl. Phys. Lett.* **89**, 113121 (2006).

<sup>11</sup>J. Tamayo, *J. Appl. Phys.* **97**, 044903 (2005).

<sup>12</sup>P. Gleyzes, P. K. Kuo, and A. C. Boccara, *Appl. Phys. Lett.* **58**, 2989 (1991).

<sup>13</sup>R. Garcia and R. Perez, *Surf. Sci. Rep.* **47**, 197 (2002).

<sup>14</sup>D. E. Oates, S. H. Park, and G. Koren, *Phys. Rev. Lett.* **93**, 197001 (2004).

<sup>15</sup>D. B. Haviland, D. Platz, and E. A. Tholén, Patent Pending (2007).

<sup>16</sup>D. Pesen, A. Erlandsson, M. Ulfendahl, and D. B. Haviland, *Lab Chip* **7**, 1603 (2007).

<sup>17</sup>W. F. Heinz and J. H. Hoh, *J. Chem. Educ.* **82**, 695 (2005).

<sup>18</sup>J. P. Cleveland, B. Anczykowski, A. E. Schmid, and V. B. Elings, *Appl. Phys. Lett.* **72**, 2613 (1998).